Charmed Particles in CORSIKA

D. Heck

Institut für Kernphysik

Forschungszentrum Karlsruhe

in der Helmholtz-Gemeinschaft

Wissenschaftliche Berichte

FZKA 7366

Charmed Particles in CORSIKA

D. Heck

Institut für Kernphysik

Abstract

Charmed Particles in CORSIKA

This report describes how the production, transport, and decay of charmed particles as well as the leptons of the third generation ($\tau^{\pm}$-leptons and ν_τ rsp. $\bar{\nu}_\tau$-neutrinos) have been added to the CORSIKA air shower simulation program.

Zusammenfassung

Teilchen mit Charm in CORSIKA

Dieser Bericht beschreibt, wie die Produktion, der Transport und der Zerfall von Teilchen mit Charm ebenso wie der von Leptonen der dritten Generation ($\tau^{\pm}$-Leptonen und ν_τ bzw. $\bar{\nu}_\tau$ Neutrinos) in das Luftschauer-Simulationsprogramm CORSIKA eingebaut wurden.

Contents

1 Introduction

Since several years there is increasing evidence that none of the hadronic interaction codes coupled with CORSIKA [1] is able to describe correctly the number and energy spectrum of muons observed in air shower experiments, especially of the muons with energies above the 100 GeV range [2, 3, 4, 5, 6, 7, 8]. It has been suspected [9], that part of this discrepancy has to be attributed to the missing production of charmed hadrons in the simulations. Therefore the new option CHARM has been introduced into CORSIKA. This option treats charmed hadrons as particles in the shower cascade generated by those interaction models which are programmed in a manner to produce them explicitly. In the standard version, this production of charmed particles is suppressed (as in QGSJET01c [10]) or the charmed hadrons decay immediately at the interaction vertex without being transported (as in DPMJET II.55 [11]).

Another topic not implemented in the previous CORSIKA versions is the handling of τ-leptons which is needed for the description of so called double-bang showers initiated by high-energy ν_τ-neutrinos (see section 3). If those neutrinos interact via a charged current exchange a τ-lepton is produced in the first bang (because of lepton number conservation). This short-lived τ-lepton consecutively decays and produces the second bang. Therefore in the CHARM option described in this report the handling of the $\tau^\pm$-leptons is included.

The decay of these particles newly introduced into CORSIKA is performed by the PYTHIA [12] routines which have to be coupled with CORSIKA.

2 τ-Leptons

The τ-leptons are generally not produced in the hadronic interaction models coupled with CORSIKA with exception of HERWIG [13] and PYTHIA [12]. Within CORSIKA the HERWIG routines are only employed to treat neutrino primaries (with the NUPRIM option) and, in the case of ν_τ-primaries a τ-lepton is generated by a charged current interaction. With the CHARM option the decay of such a τ-lepton is handled consistently by the PYTHIA routines.

2.1 τ-Lepton Cross-Sections

For the range calculation of τ-leptons, their half-life is considered as well as the three types of interaction: bremsstrahlung, pair production, and nuclear interaction are calculated in full analogy with the treatment of the muon-induced interactions.

The cross-sections for these processes are initialized in the subroutine *MUPINI*, after calculation of the muon cross-sections. All the arrays *BREMSTAB*, *PAIRTAB*, and *NUCTAB* carrying the relevant muon cross-section tables, as well as the functions *CBRSGM*, *CPRSGM*, and *CNUSGM* corresponding with these cross-sections have been extended by an additional dimension which indicates the type of the interacting
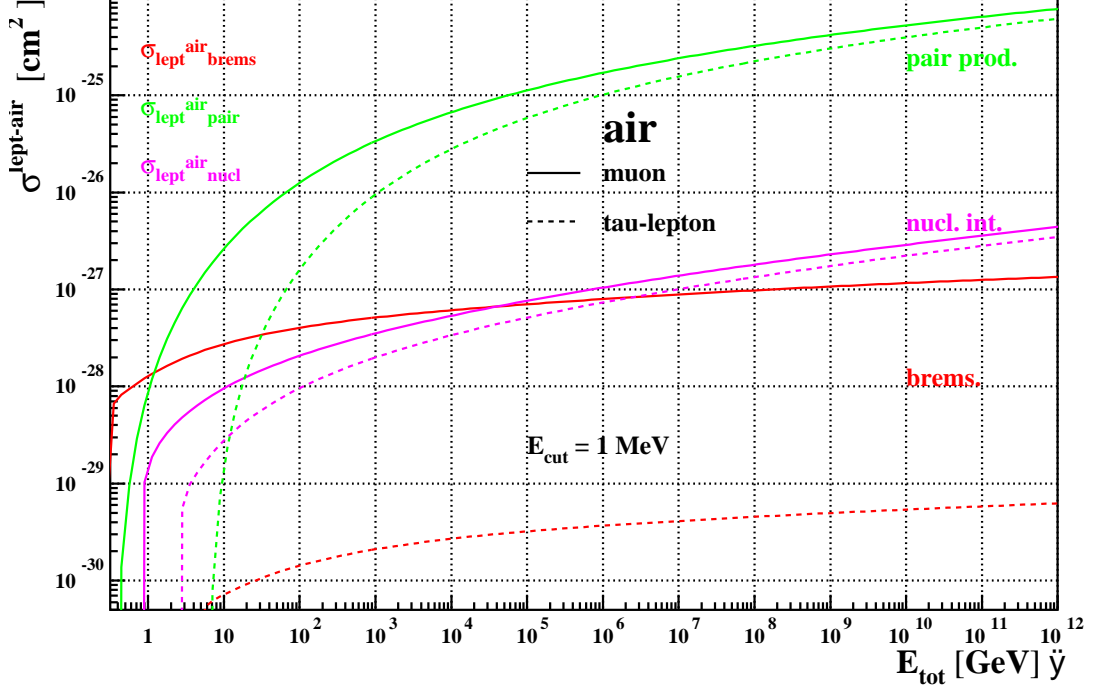
Figure 1: Interaction cross-sections with air for muons (full lines) and τ-leptons (dashed lines) as function of total energy.

lepton by the value of the index MT. The muon is indicated by 1, while the value 2 stands for the τ-lepton. In similar manner the arrays *DEDXMUB*, *DEDXMUP*, and *DEDXMNI* are extended to contain now the energy loss tables for the various processes of the τ-leptons additionally to the muonic ones. The functions *DKOKOI*, *DKOKOS*, *VBSE*, *VBSS*, *VPHL*, and *VPHM* to be used for the integration of the differential interaction cross-sections are extended by the index MT (stored in COMMON /CRMUPART/) which indicates their use for muons (MT = 1) rsp. τ-leptons (MT = 2).

The formulas for the calculation of the cross-sections are given in Ref. [14] respecting the different lepton masses of the muon and τ-lepton. In the pair production process, the transferred energy must be distributed onto the e^+e^- pair. An improved sampling of Kokoulin and Bogdanov [15] is employed for the pair creation process of muons as well as for τ-leptons. Also the energy loss by ionization is implemented for the τ-leptons in the same manner as for muons at all occasions where the range limitation by ionization energy loss comes in, such as in the subroutines *PRANGC*, *PRANGE*, *UPDATE*, and *AUGCUT*. This ionization energy loss includes the Sternheimer density effect [16] using the parameterization of Ref. [15].

The resulting cross-sections for air as function of the lepton energy are plotted in

Fig. 1. Remarkable is the large difference in the cross-sections for bremsstrahlung between the muon and the τ-lepton which amounts to more than two orders of magnitude. This large ratio is expected as this cross-section scales with the ratio of the masses $(m_\mu/m_\tau)^2 \simeq 1/283$. The cross-sections for pair production and nuclear interaction differ only at the low-energy end where the differences in the lepton rest masses play a more dominant role.

The routines for bremsstrahlung (*MUBREM*), nuclear interaction (*MUNUCL*), and pair production (*MUPRPR*) perform the interactions of the μ- and τ-lepton and are called from the routine *MUTRAC*. The decay of the τ-leptons is simulated by a call to the subroutine *CHRMDC* which serves as a link routine to the PYTHIA package [12].

3 Treatment of τ-Neutrinos

The production of secondary τ-particles (τ-leptons and the corresponding ν_τ-neutrinos) is omitted in all high-energy and low-energy hadronic interaction codes. But as ν_τ-neutrinos may come from cosmic sources their treatment as primary particles must be possible. For this purpose the NUPRIM option is available which couples the HERWIG code [13] to treat such primary neutrinos in CORSIKA. The ν_τ-neutrinos may undergo interactions with exchange of charged current (CC) producing a τ-lepton or with neutral current (NC) keeping the ν_τ-neutrino. Thus in both cases the lepton number is conserved, but part of the primary energy is transferred to the collision partner which leads to the formation of a shower. In the case of the CC-interaction the produced τ-lepton will decay because of its short live time ($\tau \approx 2.9 \cdot 10^{-13}$ sec) thus producing a second shower at some distance from the origin of the first shower. Both showers together form the typical signature of a so called 'double bang'. Therefore, for a correct description of the CC-interactions, the NUPRIM option should be combined with the CHARM option to treat the resulting τ-lepton by the PYTHIA routines. It has been tested that by coupling both packages with CORSIKA simultaneously no complications between the HERWIG and PYTHIA packages occur by duplicate names of common blocks, functions, or routines.

4 Charmed Hadrons

At the time of the implementation of the CHARM option only the interaction codes QGSJET01c [10] and the DPMJET II.55 [11, 17] are suited to produce hadrons with a charmed quark or anti-quark. In principle also the EPOS code [18] is designed to produce charmed hadrons, but at present the fourth (charmed) quark is not activated and most parameters are fine-tuned to experimental findings to take over the influence of the missing fourth quark. Therefore the activation of the fourth (charmed) quark within the code needs a careful check and readjustment of most model parameters to bring the

description of all observed secondary particles into the same level of agreement with the available experimental findings as with the production of the charm flavor switched off.

The QGSJET01c model produces only the charmed mesons and baryons with the lowest mass. These are the charged and neutral D and $\overline{D}$-mesons and the Λ_c and $\overline{\Lambda}_c$-baryons. They are used as representatives for all the higher mass charmed hadrons. Higher mass charmed hadrons are not produced in QGSJET01c.

The transport distance of the charmed hadrons to the point of decay is determined in the subroutine $BOX2$ which has been extended in analogy with that portions of this subroutine which evaluate the transport lengths of other instable particles. For the charmed hadrons the interaction cross-sections are not sufficiently well known. As their life times are generally short (the charmed hadrons with the longest half-life of $\simeq 1 \cdot 10^{-12}$ sec are the charged D^+ and $\overline{D}^-$-mesons) the interactions of charmed hadrons will play only a minor role. In test simulations, therefore, the $\pi^{\pm}$-meson rsp. nucleon cross-sections with air have tentatively been used for the charmed hadrons in QGSJET01c. The results are compared in section 5.2 with simulations in which interactions of charmed hadrons are disregarded.

In DPMJET II.55 charmed projectiles are not admitted, therefore the interaction of charmed hadrons is suppressed in favour of the decay (by setting the FDECAY flag in subroutine BOX2). For the decay at the end of the transport distance the PYTHIA routines [12] are called via the linking routine $CHRMDC$ to perform the generation of the decay products of the charmed hadrons. It should be noted that together with DPMJET II.55 only the linking with the older PYTHIA 6.1 routines gives a correctly working executable program. In the standard installation of CORSIKA + DPMJET II.55 the production of charmed hadrons is switched on, but these hadrons decay immediately at the vertex of their origin. To see the influence of the charm production, in a specialized run the charm production is suppressed by setting its production probability to zero. The results of the different test runs are compared in section 5.

5 Example

This chapter gives an example of the influence of charmed hadrons on various observable shower quantities. Generally in an inelastic collision with the nucleus of an air molecule the production of charmed hadrons is rather low. It increases with energy, so that at a projectile energy (lab) of about 10^{17} to 10^{18} eV about one charmed hadron is produced in average in a p-^{14}N-collision. Nevertheless this production might be important in air showers because of the increased production of high-energy muons. The D-mesons predominantly decay to K-mesons. Moreover charged D-mesons produce muons via a 7% branch of the decay $D^+ \rightarrow \overline{K}^0 \mu^+ \nu_\mu$ and similarly the neutral D-mesons decay in a 3.2% branch according with $D^0 \rightarrow K^- \mu^+ \nu_\mu$. Therefore in cosmic air showers some muons with very high energies stemming from charmed meson decays might be expected to arrive at ground. Other changes will be of minor importance and very

difficult to observe. As the free transport path of the charmed particles is explicitly implemented an elongation of the longitudinal distribution must be checked.

At the time of writing this report the EPOS model with explicit charm production has not been available, only the QGSJET01c model and the DPMJET II.55 code (with slight modifications [17] introduced by its author for improved charm production) could be tested with the CHARM option of CORSIKA. These tests included runs with the CORSIKA INTTEST option at different energies up to 10^{20} eV. Moreover several sets of showers induced by primary protons with vertical incidence at a primary energy of 10^{19} eV have been simulated with the QGSJET01c [10] and DPMJET II.55 [17] codes for the situation of the Auger experiment [19]. These sets of 100 showers each were calculated with rsp. without the inclusion of the explicit treatment of charmed hadrons. Also a set of showers with enabled interaction of charmed projectiles has been generated for QGSJET01c. For DPMJET II.55, in a special run the production of charmed particles has been completely inhibited by setting the charm production probability artifically to zero.

5.1 Production Rate of Charmed Hadrons

In QGSJET01c the charmed hadron production is performed via the string fragmentation, in which the charmed quarks of a $c\bar{c}$-pair from the sea (vacuum) are coupled to the quarks of the hadronizing strings of soft or semi-hard jets. This process increases rapidly with increasing energy ($\sigma = 39$ μb at $E_{lab} = 200$ GeV to $\sigma = 24$ mb at $E_{lab} = 10^{10}$ GeV for pp-collisions [20]). Depending on the partner of the charmed quark a charmed meson (in the case of an ordinary quark partner) or a charmed baryon (in the case of a coupling diquark) is produced. An additional contribution to the charmed hadron production comes from the leading nucleon conversion into a leading Λ_cD-pair. The cross-section for this conversion amounts in pp-collisions in QGSJET01c to $\sigma = 25$ μb at $E_{lab} = 200$ GeV, but rises only gradually to $\sigma = 310$ μb at $E_{lab} = 10^{10}$ GeV, thus becoming less important at the highest energies [20]. The production cross-sections and kinematic parameters for the secondary charmed hadrons as simulated in the QGSJET01c program have recently been examined in detail in Ref. [21].

In DPMJET II.55 we have three different mechanisms which are responsible for the charmed hadron production [17, 22]:

a) Inside the chain decay,

b) at the ends of soft sea chains, and

c) at the ends of hard and semi-hard chains (mini-jets).

The first contribution comes from the fragmentation of strings which is treated in DPMJET by the PYTHIA model. But in DPMJET an enhanced $c\bar{c}$-probability near a valence diquark at the end of diquark-quark or a diquark-antidiquark chains is not neglected, an effect demonstrated in fixed-target experiments [25] and referred to as *leading quark effect* [26]. Only the third mechanism relies on a solid theoretical basis of
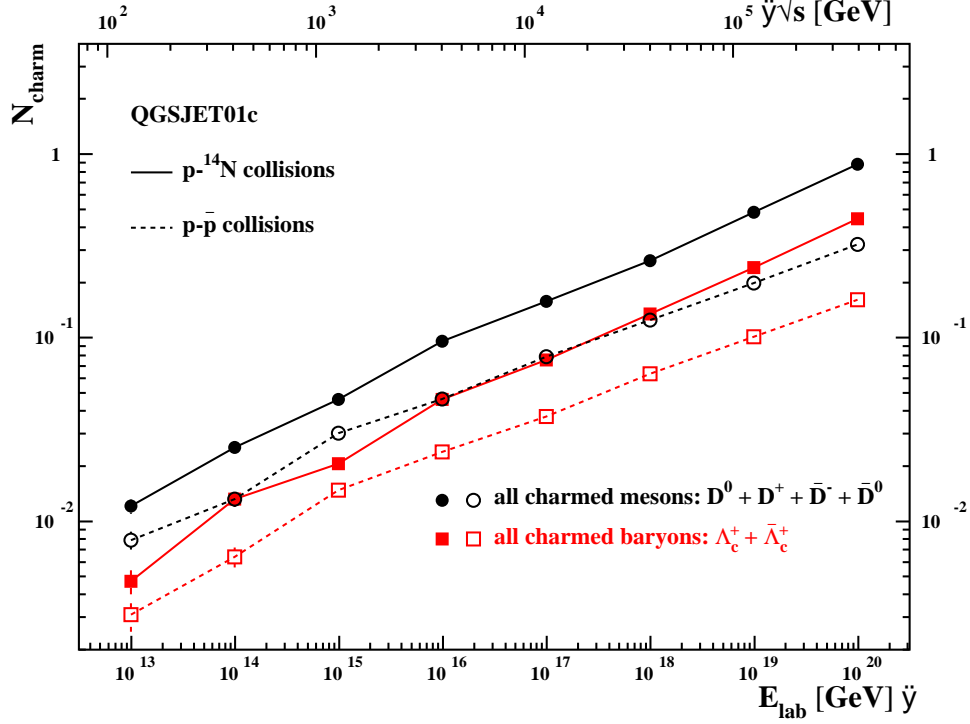
Figure 2: Average production rates of charmed mesons (black curves, circular dots) and charmed baryons (red curves, squared dots) for p-^{14}N-collisions (solid lines) and p$\bar{\text{p}}$-collisions (dashed lines) in QGSJET01c.

perturbative Quantum ChromoDynamics and is the dominant contribution in hadronic and nuclear collisions at energies (lab) above the TeV range. The other two mechanisms are introduced phenomenologically for the charm and prompt muon production within cosmic ray induced air showers.

With the INTTEST option of CORSIKA for interaction tests the production of charmed hadrons in p-air and p$\bar{\text{p}}$-collisions is examined. The production rates averaged over 10000 collisions at each energy value are given in Fig. 2 for QGSJET01c and in Fig. 3 for DPMJET II.55.

The resulting rates of QGSJET01c from p$\bar{\text{p}}$-collisions have to be compared with findings of Ref. [21] accounting for the fact that in Ref. [21] the four meson and two baryon species are considered individually, while in the CORSIKA INTTEST option only the summed production rates for charmed mesons and charmed baryons are available. A good agreement for the p$\bar{\text{p}}$-collisions with Ref. [21] is observed.

For DPMJET II.55 in Fig. 3 an approximate agreement with Fig. 2 is found only for the charmed baryons from p$\bar{\text{p}}$-collisions, while the contribution of charmed mesons is higher by a factor of ≈ 4 relative to QGSJET01c. More pronounced are the differences in p-^{14}N-collisions: For DPMJET II.55 the number of charmed baryons is typically higher by a factor of ≈ 2 relative to QGSJET01c, while the charmed mesons rise above
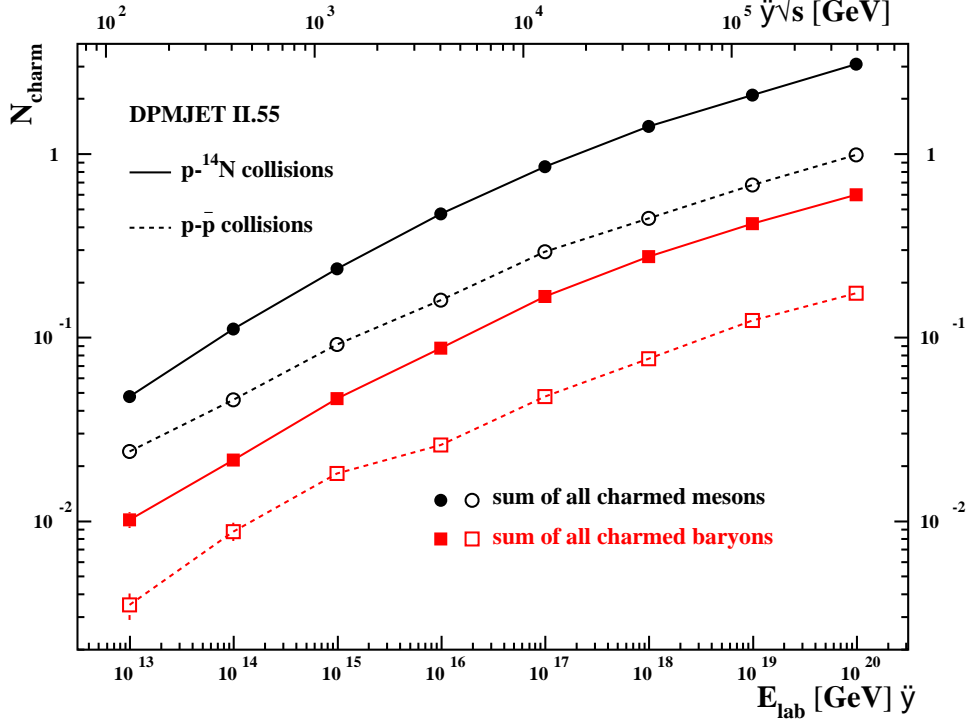
Figure 3: Average production rates of charmed mesons (black curves, circular dots) and charmed baryons (red curves, squared dots) for p-^{14}N-collisions (solid lines) and p$\bar{\text{p}}$-collisions (dashed lines) in DPMJET II.55.

those from QGSJET01c by a factor of ≈ 5.

5.2   Muon Energy Spectra

The energy spectra of muons arriving at the observation level in an altitude of 1452 m (Auger location [19]) are compared in Fig. 4 for different runs with QGSJET01c and in Fig. 5 for runs with DPMJET II.55. The kinetic energy of muons is given on the abscissa of the plots. A detailed analysis indicates that muons with energies above 100 TeV arrive within a distance of < 1 m from the shower axis.

For QGSJET01c the three plotted cases of Fig. 4 comprise:

a) With inclusion of charmed hadrons with transport during their life time, but only decaying,

b) with inclusion of decaying charmed hadrons and including their interactions, and

c) with the charm production switched off completely in the interaction models (by a different parameter set in QGSJET01c and suppressed production probability in DPMJET II.55).
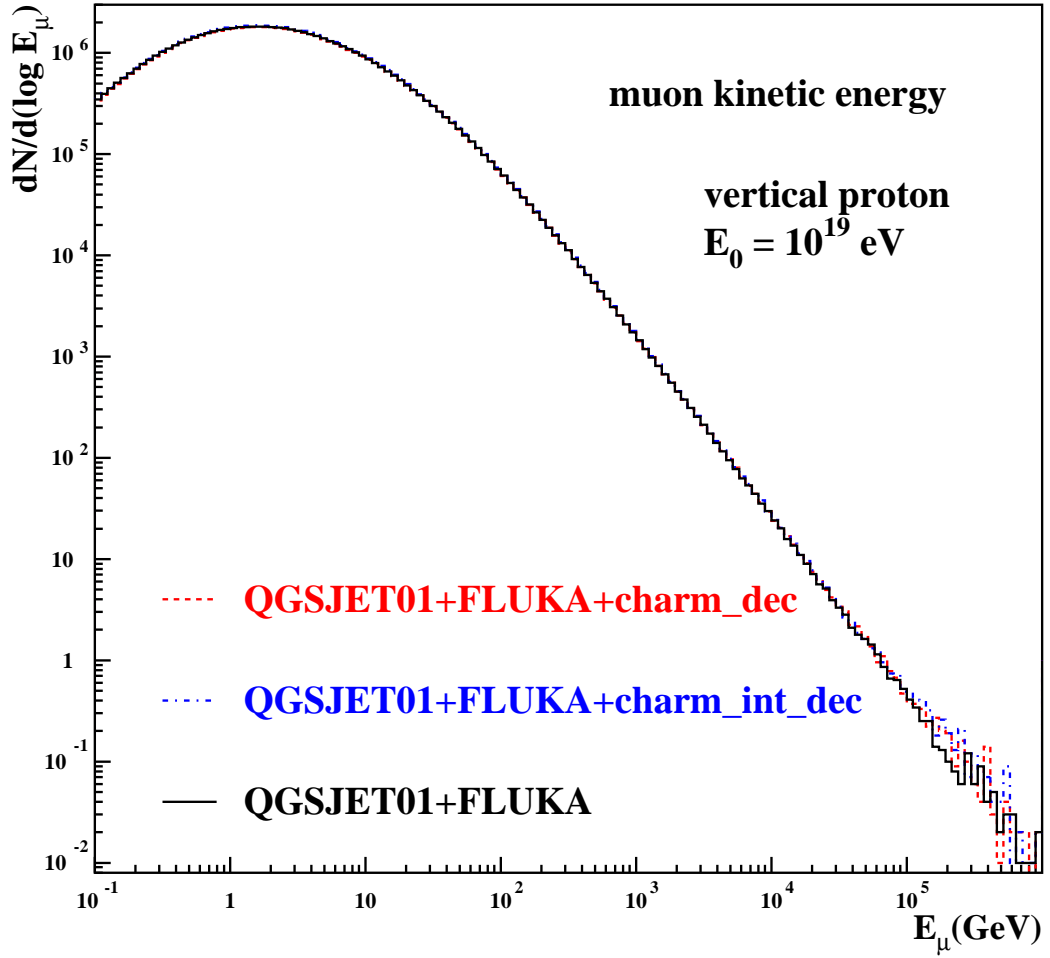
Figure 4: Muon energy spectrum with inclusion of decaying charmed hadrons (dashed line in red), with decaying and interacting charmed hadrons (dotted-dashed line in blue), and without production of charmed hadrons (full line in black) for QGSJET01c. For the low-energy interaction model ($E_{lab} < 200$ GeV) the FLUKA model [23] has been used.
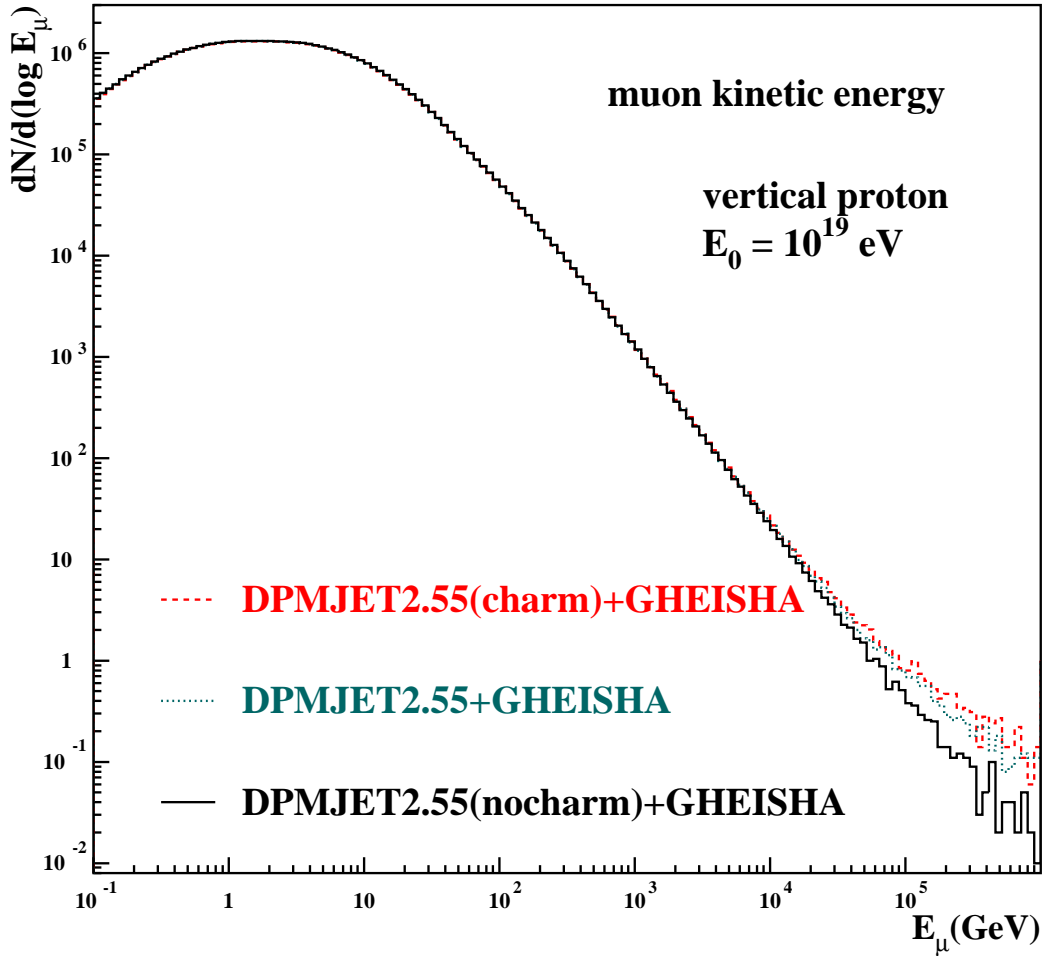
Figure 5: Muon energy spectrum with inclusion of charmed hadrons decaying after transport during their lifetime (dashed line in red), decaying immediately at the production vertex (dotted line in green), and with artificial suppression of charm production (full line in black) for DPMJET II.55. For the low-energy interaction model ($E_{lab} < 80$ GeV) the GHEISHA model [24] has been used.

Differences show up only at the high-energy end of the muon spectra at energies above 100 TeV. As expected the muon energy spectrum is significantly enhanced in the case of decaying charmed hadrons without their interaction and is only slightly enhanced in the case of respecting the interaction of charmed hadrons. But the numbers of such high-energy muons are extremely low as, on average, less than one muon with $E_\mu > 100$ TeV arrives per shower at the observation level.

For DPMJET II.55 the Fig. 5 shows the three cases

a) With charmed hadrons with decay after transported during their life time,

b) with charmed hadrons decaying immediately at the production vertex, and

c) with the charm production suppressed in the interactions.

Again the largest enhancement of the high-energy muons is observed for the case of the decaying charmed hadrons. If the decaying charmed hadrons are not transported during their life time, but decay at the vertex (case b)), the enhancement is slightly reduced.

As in DPMJET II.55 the production of charm without transport is the standard case, a set of showers has been produced with artificial blocking the charm production shown as case c). This blocking [1] gives a result well to be compared with the case c) of QGSJET01c shown in Fig. 4. A careful comparison of Fig. 4 with Fig. 5 reveals a slight difference at muon energies around 1 to 10 GeV. This difference is caused by the different low-energy hadronic interaction models (FLUKA vs. GHEISHA) used in the two sets of simulations.

5.3 Longitudinal Distributions

With the additional muons coming from charmed particle decay after the first hadronic interactions one might suppose that the longitudinal development of an air shower might be altered by respecting the transported charmed hadrons. This is examined carefully. CORSIKA samples not only the charged particle longitudinal distribution, but also the energy deposit longitudinal distribution which best reflects the expected air fluorescence signal along the shower axis which is measured e.g. in the fluorescence detectors of the Auger experiment [19]. For both types of longitudinal distributions the maxima of the sets of simulated showers (each set with 100 showers induced by vertically incident protons with 10^{19} eV) have been determined and collected in Table 1. It shows that all 6 values of QGSJET01c and correspondingly of DPMJET II.55 differ only slightly and coincide well within the error bars, i.e. a significant influence of the charmed hadron production on the longitudinal distributions is not observed.

---

[1]The blocking is achieved by setting PCCC within subroutine XPTFL and setting PC within subroutines XPTFL1, FLKSAA, DIQSV, DIQVS, DIQDSS, DIQSSD, DIQDZZ, and DIQZZD to zero.

Table 1: Maxima of longitudinal distributions (Each item represents the average of 100 showers induced by vertically incident protons of 10^{19} eV).

Interaction model configuration	Maximum of longitudinal distribution	
	charged particles [g/cm^2]	energy deposit [g/cm^2]
QGSJET+FLUKA+charm_dec	776.86 ± 7.32	771.28 ± 7.23
QGSJET+FLUKA+charm_dec_int	773.31 ± 9.19	771.41 ± 7.42
QGSJET+FLUKA	773.02 ± 7.58	775.74 ± 7.80
DPMJET(charm)+GHEISHA	818.49 ± 7.94	819.51 ± 6.47
DPMJET+GHEISHA	818.60 ± 6.96	823.57 ± 7.20
DPMJET(nocharm)+GHEISHA	819.93 ± 8.29	821.11 ± 7.46

6   Final Remarks

From the example shown in the previous section on might conclude:

- The inclusion of explicit charm production in simulations gives no significant differences for most observable shower parameters.

- As expected, the number of 'direct' muons with energies above 100 TeV is slightly increased by the charm production. But the observed number of extra muons depends strongly on the used high-energy hadronic interaction model and on the treatment of the produced charmed hadrons.

- Further tests with the EPOS model may help to clarify the different rates of charmed mesons and charmed baryons observed for the QGSJET01c and DPM-JET II.55 models. These different production rates are reflected by the different numbers of extra high-energy muons.

A Considered Particles in the CHARM Option and Particle Codes

In the CHARM option a series of unstable particles is specified in CORSIKA by their mass and life time. The charmed hadrons are grouped into the charmed mesons and the charmed baryons. A third group contains the leptons of the third generation.

In the four 'normal' charmed mesons one quark (anti-quark) is replaced by a charmed quark (charmed anti-quark) (identification codes 116 - 119). The strange charmed mesons are composed of a strange quark and a charmed quark (identification codes 120 - 121). Finally the η_c meson is composed of a charmed quark-anti-quark pair (identification code 122). For all these charmed mesons, their first excited states are defined (identification codes 123 - 126, 127 - 128, 130).

In the simplest charmed baryons, one quark (anti-quark) is replaced by a charmed quark (anti-quark) (identification codes 137, 140 - 142, 149, 152 - 154), the excited states of these baryons are included (identification codes 161 -163, 171 - 173). Replacing one quark by a strange quark and a second by a charmed quark leads to the Ξ_c baryons and anti-baryons (identification codes 138 - 139, 150 - 151) and their excited states (identification codes 143 - 144, 155 - 156). If a second u- or d-quark is replaced by a strange quark we have the Ω_c (identification code 145, 157).

The third group of new particles in CORSIKA contains the members of the third lepton generation, which are the τ-lepton (identification codes 131 - 132) and the ν_τ-neutrino (identification codes 133 - 134).

The identification codes of the newly defined particles used in CORSIKA and in the different interaction codes are listed in Table 2. In CORSIKA, for all those particles, the identification codes coincide with those of DPMJET II.55 [11], but not all particles available in DPMJET are also available in CORSIKA. The identification codes of PYTHIA [12] and HERWIG [13] are in agreement with the recommendations of the Particle Data Group [27]. The particle codes of EPOS [18] correspond with those of the program ISAJET [28]. This numbering is also used in the programs NEXUS [29] and VENUS [30].

Table 2: Charmed particles used in CORSIKA (to be continued).

Particle identifications						
Particle name	Particle mass [GeV]	Particle life time [sec]	Identification code			
			CORSIKA DPMJET	PYTHIA HERWIG (PDG)	EPOS (ISAJET)	QGSJET
D°	1.8645	$4.101*10^{-13}$	116	421	-140	8
D^+	1.8697	$1.040*10^{-12}$	117	411	-240	7
$\overline{D}^-$	1.8697	$1.040*10^{-12}$	118	-411	240	-7
$\overline{D}^{\circ}$	1.8645	$4.103*10^{-13}$	119	-421	140	-8
D_s^+	1.9682	$5.00*10^{-13}$	120	431	-340	
$\overline{D_s}^-$	1.9682	$5.00*10^{-13}$	121	-431	340	
η_c	2.9804	$3.805*10^{-23}$	122	441	440	
$D^{*\circ}$	2.0067	$4.*10^{-22}$	123	423	-141	
D^{*+}	2.0100	$6.86*10^{-21}$	124	413	-241	
$\overline{D^*}^-$	2.0100	$6.86*10^{-21}$	125	-413	241	
$\overline{D^*}^{\circ}$	2.0067	$4.*10^{-22}$	126	-423	141	
D_s^{*+}	2.1121	$4.*10^{-22}$	127	433	-341	
$\overline{D_s^*}^-$	2.1121	$4.*10^{-22}$	128	-433	341	
J/ψ	3.096916	$7.233*10^{-21}$	130	443	441	
τ^+	1.77699	$2.906*10^{-13}$	131	-15	-16	
τ^-	1.77699	$2.906*10^{-13}$	132	15	16	
ν_τ	0.	stable	133	16	15	
$\overline{\nu}_\tau$	0.	stable	134	-16	-15	
Λ_c^+	2.28646	$2.00*10^{-13}$	137	4122	2140	9
Ξ_c^+	2.4679	$4.42*10^{-13}$	138	4232	3140	
Ξ_c°	2.4710	$1.12*10^{-13}$	139	4132	3240	
Σ_c^{++}	2.45402	$2.95*10^{-22}$	140	4222	1140	
Σ_c^+	2.4529	$2.*10^{-22}$	141	4212	1240	
Σ_c°	2.45376	$3.*10^{-22}$	142	4112	2240	
$\Xi_c'^+$	2.5757	$1.*10^{-23}$	143	4322	1340	
$\Xi_c'^{\circ}$	2.5780	$2.*10^{-22}$	144	4312	2340	
Ω_c°	2.6975	$6.9*10^{-14}$	145	4332	3340	

Table 2: (continued) Charmed particles used in CORSIKA.

Particle identifications (continued)						
Particle name	Particle mass [GeV]	Particle life time [sec]	Identification code			
			CORSIKA DPMJET	PYTHIA HERWIG (PDG)	EPOS (ISAJET)	QGSJET
$\overline{\Lambda_c}^-$	2.28646	$2.00*10^{-13}$	149	-4122	-2140	-9
$\overline{\Xi_c}^-$	2.4679	$4.42*10^{-13}$	150	-4232	-3140	
$\overline{\Xi_c}^\circ$	2.4710	$1.12*10^{-13}$	151	-4132	-3240	
$\overline{\Sigma_c}^{--}$	2.45402	$2.95*10^{-22}$	152	-4222	-1140	
$\overline{\Sigma_c}^-$	2.4529	$2.*10^{-22}$	153	-4212	-1240	
$\overline{\Sigma_c}^\circ$	2.45376	$3.*10^{-22}$	154	-4112	-2240	
$\overline{\Xi'_c}^-$	2.5757	$1.*10^{-23}$	155	-4322	-1340	
$\overline{\Xi'_c}^\circ$	2.5780	$1.*10^{-23}$	156	-4312	-2340	
$\overline{\Omega_c}^\circ$	2.6975	$6.9*10^{-14}$	157	-4332	-3340	
Σ_c^{*++}	2.5184	$3.66*10^{-23}$	161	4224	1141	
Σ_c^{*+}	2.5175	$4.*10^{-23}$	162	4214	1241	
$\Sigma_c^{*\circ}$	2.5180	$5.06*10^{-23}$	163	4114	2241	
$\overline{\Sigma_c^*}^{--}$	2.5184	$3.66*10^{-23}$	171	-4224	1141	
$\overline{\Sigma_c^*}^-$	2.5175	$4.*10^{-23}$	172	-4214	1241	
$\overline{\Sigma_c^*}^\circ$	2.5180	$5.06*10^{-23}$	173	-4114	2241	

B   Link Routines to PYTHIA

The modifications and additions to calculate the τ-lepton cross-sections have already been briefly described in Sect. 2.1. Moreover for a correct treatment of the charmed particles a series of modifications have been performed and several new routines have been added.

B.1   Modified Routines

- *BOX*2: The calculation of the free path to the first interaction of primary ν_τ-neutrinos is performed as for the primary ν_e and ν_μ-neutrinos. The τ-lepton range calculation and fate determination (bremsstrahlung, pair production, nuclear interaction, decay) follows that of the muons.
  The range calculation for the (instable) charmed hadrons is performed in analogy with the other mesons or instable baryons. Only in test runs with QGSJET01c[2] the cross-sections of charmed pions are assumed for the charmed mesons and those of the nucleons for the charmed baryons. For those interaction codes (DPMJET, EPOS) which are not able to treat charmed projectiles the decay flag FDECAY is activated to prevent a later interaction at the end of the transport distance.

- *MUTRAC*: In dependence on the index MT indicating a muon (MT=1) or a τ-lepton (MT=2) the decay routines *MUDECAY* (for muons) rsp. *CHRMDC* (for τ-leptons) are called. *CHRMDC* acts as a link routine to the PYTHIA package.

- *NUCINT*: The selection of interaction rsp. decay routines in dependence on the projectile type is extended for the charmed hadrons. In the case of decay a call to the new routine *CHRMDC* is performed. The *CHRMDC* routine acts as a link routine to the PYTHIA package to treat the charmed particle decays.

- *PAMAF*: The mass and life time tables of the new particles are initialized additionally to the already existing ones.

- *TSTACK*: The energy check of secondary particles (before shifting them on the particle stack) is extended to the charmed hadrons and to the leptons of the third generation.

- *DPMDAT*, *DPMJIN*, *DPMJST*: The immediate decay of charmed secondary hadrons at the interaction vertex is suppressed, rather those secondaries are copied to the CORSIKA stack for further transport. The conversion of the PDG particle code (used in the output files of *DPMJET*) to the particle identification

---

[2]It should be noted that in QGSJET01c in the case of charmed projectiles the charmed quark is not conserved in the interaction which leads to an underestimation in the influence of charm on the number of high-energy muons.

used in CORSIKA has been extended for the charmed hadrons and the leptons of the third generation.

- *HERDAT*: The list of particles recognized by CORSIKA has been extended.

- *NEXLNK*, *NSTORE*: These routines used by EPOS are extended to enable a treatment of charmed particles.

- *QGSDAT*, *QGSINI*: These routines are enabled for those charmed hadrons which are listed in the column 'QGSJET' in Table 2. The parameters DC(3) and DC(5) of the COMMON /AREA8/ are set in *QGSINI*. These two parameters determine the relative probabilities of $c\bar{c}$-pair creation in the string hadronization.

- *TST*, *HISFIL*, *HISINI*, *HISTRA*: Two new particle classes 'charmed mesons' and 'charmed baryons' have been added to the existing 25 particle classes of the interaction test (INTTEST option of CORSIKA).

B.2 New Routines

Several routines have been added to meet the requirements of linking with the PYTHIA package [12].

- *CHRMDC*: This routine is the essential link routine to the PYTHIA package. It stores the coordinates of the decay vertex to be taken over by the decay products. The PYTHIA input routine *PY1ENT* is called with the actual arguments of identification code and energy of the decaying particle.

- *PYR*: This function uses the first sequence of the CORSIKA random generator *RMMAR* to produce the random numbers for the PYTHIA package.

- *PYTDAT*: This BLOCK DATA routine contains the extended lookup table for the conversion of CORSIKA particle identifications to the PYTHIA (PDG) identifications.

- *PYTINI*: This initialization routine sets various PYTHIA parameters for warning and error printing. After initializing the PYTHIA package it disables the decay of those unstable hadrons which are treated in detail in other CORSIKA routines (*ETADEC*, *KDECAY*, *NUCINT*, *PI0DEC*, *STRDEC*) and enables the decay of charmed hadrons and $\tau^{\pm}$-leptons.

- *PYTSTO*: This subroutine performs the storage of the decay products delivered by PYTHIA into the CORSIKA stack.

References

[1] D. Heck et al., Report **FZKA 6019**, Forschungszentrum Karlsruhe (1998); http://www-ik.fzk.de/corsika/physics_description/corsika_phys.html

[2] P. Desiati et al. (AMANDA Collab.), *Proc. 27th Int. Cosmic Ray Conf.*, Hamburg, Germany (2001) 985

[3] F. Schröder et al., *Proc. 27th Int. Cosmic Ray Conf.*, Hamburg, Germany (2001) 1013

[4] V. Avati et al., *Astropart. Phys.* **19** (2003) 513

[5] J. Abdallah et al. (DELPHI Collab.), *Astropart. Phys.* **28** (2007) 273

[6] P. Achard et al. (L3 Collab.), *Phys. Lett.* **B598** (2004) 15

[7] J. Ridky, P. Travnicek, *Nucl. Phys. B* (Proc. Suppl.) **138** (2005) 295; P. LeCoultre, *Nucl. Phys. B* (Proc. Suppl.) **122** (2003) 161

[8] T. Antoni et al. (KASCADE Collab.), *Astropart. Phys.* **24** (2005) 1

[9] J. Ridky et. al., *Proc. 30th Int. Cosmic Ray Conf.*, Mérida (México), HE 1.6, contr. 812 (2007); *arXiv:astro-ph/* 0706.2145 (2007)

[10] N.N. Kalmykov, S.S. Ostapchenko, A.I. Pavlov, *Nucl. Phys. B (Proc. Suppl.)* **52B** (1997) 17; S.S. Ostapchenko, private communication (2007)

[11] J. Ranft, *arXiv:hep-ph/* 9911213 and *arXiv:hep-ph/* 9911232 (1999)

[12] T. Sjöstrand, S. Mrenna, P. Skands, Report **LU TP 06-13** (2006); *arXiv:hep-ph/* 0603175 (2006)

[13] G. Corcella et al., *JHEP* **0101** (2001) 010; G. Marchesini et al., *Comp. Phys. Comm.* **67** (1992) 465; http://hepwww.rl.ac.uk/theory/seymour/herwig/

[14] S. Bottai, L. Perrone, *Nucl. Instr. Meth.* **A 459** (2001) 319

[15] R.P. Kokoulin, A.G. Bogdanov, private communication (2007)

[16] R.M. Sternheimer, M.J. Berger, S.M. Seltzer, *Atomic Data and Nuclear Data Tables* **30** (1984) 261

[17] P. Berghaus, T. Montaruli, J. Ranft, *Journal of Cosmology and Astroparticle Physics*, **0806** (2008) 003; *arXiv:astro-ph/* 0712.3089 (2007)

[18] K. Werner, F. M. Liu, T. Pierog, *Phys. Rev.* **C 74** (2006) 044902; T. Pierog and K. Werner, *arXiv:astro-ph/* 0611311 (2006)

[19] J. Abraham et al. (AUGER Collab.), *Nucl. Instr. Meth.* **A 523** (2004) 50

[20] N.N. Kalmykov et al., *Proc.* 24th *Int. Cosmic Ray Conf.*, Rome (Italy), Vol.**1**, 123 (1995)

[21] U. Dev Goswami, *Astropart. Phys.* **28** (2007) 251

[22] G. Battistoni et al., *Astropart. Phys.* **4** (1996) 351

[23] A. Fassò,et al., *Computing in High Energy and Nuclear Physics 2003 Conference* (CHEP2003), La Jolla, CA (USA), March 24-28, 2003 (paper MOMT005); eConf C0303241 (2003); *arXiv:hep-ph/*0306267 (2003); http://www.fluka.org/references.html

[24] H. Fesefeldt, Report **PITHA-85/02** (1985), RWTH Aachen

[25] F.G. Garcia et al. (SELEX Collab.), *Phys. Lett.* **B528** (2002) 49

[26] T. Tashiro et al., *Int. J. Mod. Phys.* **A 19** (2004) 599

[27] W.-M. Yao et al. (Particle Data Group), *J. Phys.* **G 33** (2006) 1

[28] H. Baer et al., Report **BNL-HET-99/43** (1999); *arXiv:hep-ph/* 0001086 (2000)

[29] H.J. Drescher et al., *Phys. Rep.* **350** (2001) 93

[30] K. Werner, *Phys. Rep.* **232** (1993) 87